PART I: AN UNTUNED CLOCK MECHANISM OF SPECIAL DESIGN PART II: AN EXPERIMENTAL STUDY OF THE MOTION OF AN UNTUNED CLOCK

REPORT NO. 186-5 OF WORK CARRIED OUT UNDER CONTRACT DAI-49-186-502-ORD(P)-186, SUPPLEMENTAL AGREEMENT NO. 2. FOR THE DIAMOND ORDNANCE FUZE LABORATORIES. THIS IS A CONTINUATION OF WORK DESCRIBED IN REPORTS 1 AND 2 UNDER THE ABOVE CONTRACT, AND TWO PRECEEDING REPORTS COMPLETED UNDER CONTRACT CST-1224.

VIRGINIA MILITARY INSTITUTE
DEPARTMENT OF PHYSICS
LEXINGTON, VIRGINIA

JUNE 1956

ABSTRACT OF REPORT

An untuned clock mechanism with specially designed verge faces is described. This mechanism operates in a symmetric cycle in reference to leading and trailing faces of the verge.

A study of this verge design indicates a probable minimizing of the effects of geometrical variations of the leading face, observed with normal verges.

Part II of this report represents some experimental results on the motions of verge and starwheel in the equilibrium cycle.

PART I: AN UNTUNED CLOCK MECHANISM OF SPECIAL DESIGN

I. INTRODUCTION

A thorough study of the untuned clock has been carried out in this laboratory over the past several years. Four reports are on file in the library of DOFL embodying the results of this study. The reports are titled as follows. The numbers are used for convenience in referring to these reports.

R-1: A STUDY OF THE DYNAMICS OF AN UNTUNED CLOCK MECHANISM.

R-2: A STUDY OF THE EFFECTS OF GEOMETRICAL FACTORS UPON THE BEHAVOUR OF AN UNTUNED CLOCK MECHAMISM.

R-3: A STUDY OF THE NON-UNIFORMITY IN RUNNING RATES OF A CERTAIN TYPE OF TIME DELAY MECHANISM.

R-4: THE EFFECT OF UNBALANCED VERGE TORQUES, ACCELERATION FRICTION TORQUES, AND VERGE-STARWHEEL MATERIAL UPON THE RUNNING RATES OF A CERTAIN TYPE OF TIME DELAY MECHANISM.

It has become obvious as the result of these studies that the cycle of motion for the normal verge-starwheel combination is asymmetric, due largely to the fact that the ratio u/v is changing during periods of contact between verge face and starwheel tooth. In particular $u/v < 1$ at first contact leading and increases to $u/v > 1$ at last contact. On the trailing face the opposite situation occurs.

Because of this one finds that the effect of the collision on leading face is always more pronounced or, in other words, changes in velocity are always greater at the leading face. Report R-3 indicates clearly that any geometrical changes at the leading face result in large changes in total period. On the other hand, changes at the trailing face lead to much smaller changes in running time. Cumulative evidence of this type implies that if u/v can be made constant and the same for either face a more symmetrical cycle will occur. With such a verge, it is further hoped that geometrical changes at either face will result in much less drastic changes in the running times. In this manner the importance of such geometrical changes might, on the whole, be minimized. Hence in any given group of clocks, the small geometrical variations from clock to clock will introduce variations in running rate of smaller magnitude that are now found.

II. VERGE DESIGN

Reference to the reports R-1, R-2 of the series will explain the back ground of the following discussion.

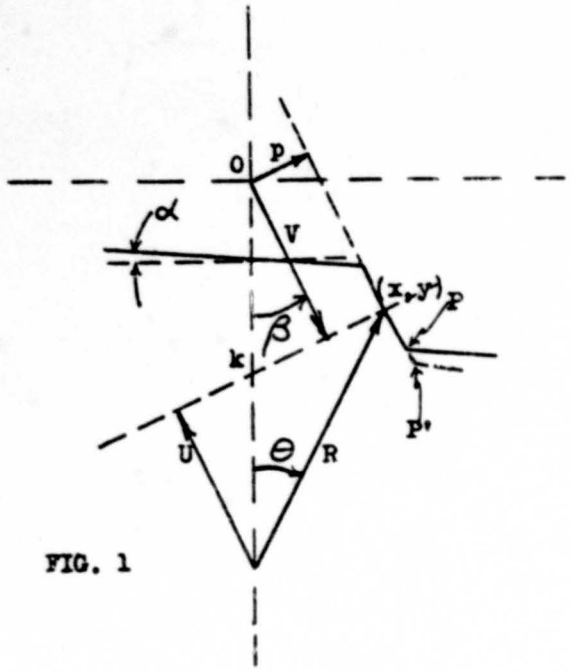

FIG. 1

We wish to design a new verge face whose shape will no longer be a straight line. Whatever this shape may be, the position of the corner point will be left unchanged. Consider first the leading face. The lever arms u and v are shown. α measures the rotation of the verge and β measures the rotation of a normal to the verge face. α is in general not equal to β.

At any point (x,y)

1) $\sin(\beta + \theta) = p/R - k \sin\beta/R \quad k<0.$

where p is the distance from O to the tangent drawn to the verge face at (x,y). We can also show that

2) $u/v = \dfrac{-R\cos(\theta+\beta)}{k\cos\beta + R\cos(\beta+\theta)}$

Taking a derivative in 1) gives

3) $\cos(\beta+\theta)\left(\dfrac{d\beta}{d\theta}+1\right) = \dfrac{1}{R}\dfrac{dp}{d\theta} - \dfrac{k}{R}\cos\beta\dfrac{d\beta}{d\theta}$

Setting u/v = C in 2) and substituting in 3)

4) $$\frac{d\beta}{d\theta} = C + \frac{1+C}{k\cos\beta}\frac{dp}{d\theta}$$

This equation indicates that at any point (x,y) $d\beta/d\theta$ can be thought of as consisting of two conponents. The first component is constant, the second depends on $dp/d\theta$. If p = const., then $dp/d\theta = 0$ and $d\beta/d\theta = C$. This is just the case for which the face of the verge is plane. We interpret $(d\beta/d\theta)_1 = C$ as that component of the rotation measured by β which is caused by the actual space rotation of the verge. The second component is that caused by the curvature of the verge face, apart from any actual verge rotation.

A logical choice for C is unity, since $u/v \simeq 1$ in the normal verge. The problem is to determine the shape of the leading verge face for which $u/v = 1$. Using equation 2), solve for β for a range of θ from .6354 to .5100 . $\theta = .6354$ is the angle of last contact leading. These values of β are substituted into equation 1) and p is computed for each θ. Now assume that as θ changes by .01 radian p will remain constant, which is physically the same as assuming that the verge surface is plane over this small interval. Suppose, for example, that at $\theta = \theta_1$, we find $\beta = \beta_1$ and $p = p_1$. Set $\theta_2 = \theta_1 + .01$, and using $p_2 = p_1$ solve for β_2'. This latter value will not be the same as the β_2 previously computed because p has not been allowed to change. The difference $\beta_2' - \beta_2 = \Delta\alpha$ is approximately that part of $\Delta\beta$ which is caused by the pure rotation of the verge. As shown above, $\frac{\Delta\alpha}{\Delta\theta} = C$, and we find on computing that $\Delta\alpha = .0103$. The discrepancy of .0003 is due to the fact that $\Delta\theta = .01$ rad. Smaller $\Delta\theta$ intervals would give better agreement.

The problem of discovering the proper shape of the face remains. The point (x_o, y_o) in Fig. 2 represents the position of last contact leading. Imagine that the tooth slides back along the verge face into some new position (x_1, y_1). The coordinates of any such point are given by

$$x = R\sin\theta$$

$$y = k + R\cos\theta$$

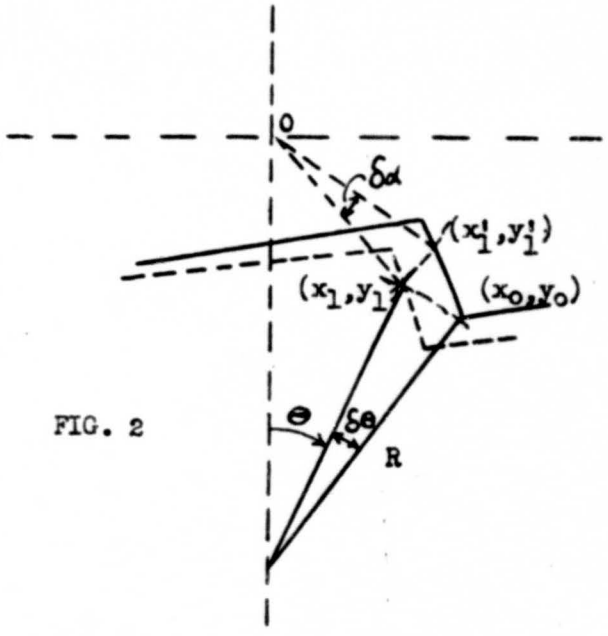

FIG. 2

At position (x_1, y_1) the verge has turned through a total angle $\delta\alpha = \Sigma\Delta\alpha$ starting from position of last contact, which corresponds to the total change $\delta\theta = \Sigma\Delta\theta$. The value $\delta\alpha$ can be readily determined from the preceding computations. Now if the verge is rotated back through this angle we can find the new coordinates of our point, (x_1', y_1'). This point, and all other such points, lies on the verge face at the position occupied at the instant of last contact. Therefore, the shape of the face for $u/v = 1$ is found by tracing through these points. This is done in Fig. 3.

For the trailing face the method of design is very nearly the same.

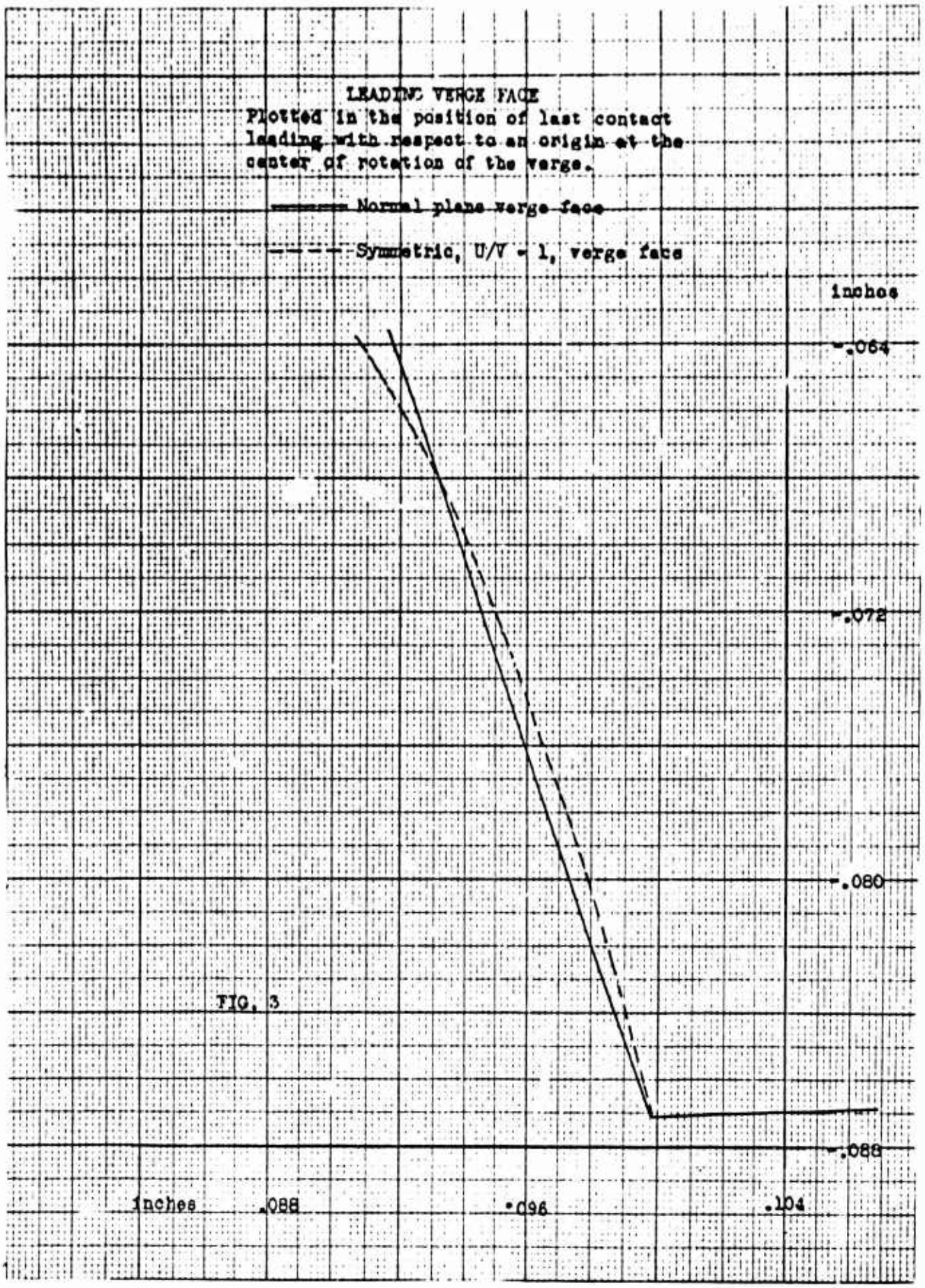
LEADING VERGE FACE
Plotted in the position of last contact leading with respect to an origin at the center of rotation of the verge.
Normal plane verge face
Symmetric, U/V = 1, verge face
inches
-.064
-.072
-.080
-.088
inches .088
.096
.104

FIG. 3

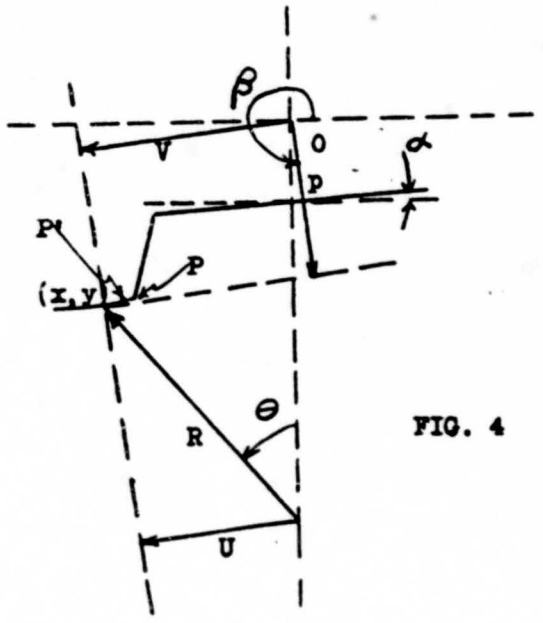

FIG. 4

Again the equation

$$5)\quad \sin(\beta + \theta) = p/R - k\sin\beta/R$$

holds at a point (x,y), where p is a function of θ. β measures the rotation of the normal to the verge face, while α will be used as a measure of true verge rotation.

Taking a derivative in equation 5) gives

$$6)\quad \frac{d\beta}{d\theta} = \frac{1/R\,\frac{dp}{d\theta} - \cos(\theta + \beta)}{\cos(\theta + \beta) + k\cos\beta/R}$$

For the leading face we have

$$7)\quad u/v = \frac{R\cos(\theta + \beta)}{k\cos\beta + R\cos(\theta + \beta)}$$

Setting u/v = 1 gives $270^\circ = \beta$. Under these circumstances 6) becomes

$$8)\quad \frac{d\beta}{d\theta} = \frac{\frac{1}{R}\frac{dp}{d\theta}}{\sin\theta} - 1$$

The term $\frac{1}{R}\frac{\frac{dp}{d\theta}}{\sin\theta}$ represents that part of the rotation of the normal to the face due solely to the change in slope of the face, since if p = constant this term equals zero. The second term is the rate at which the verge actually rotates with respect to θ. If the procedure outlined above for leading face is now followed one obtains the shape of the trailing face. Fig. 5 shows this face.

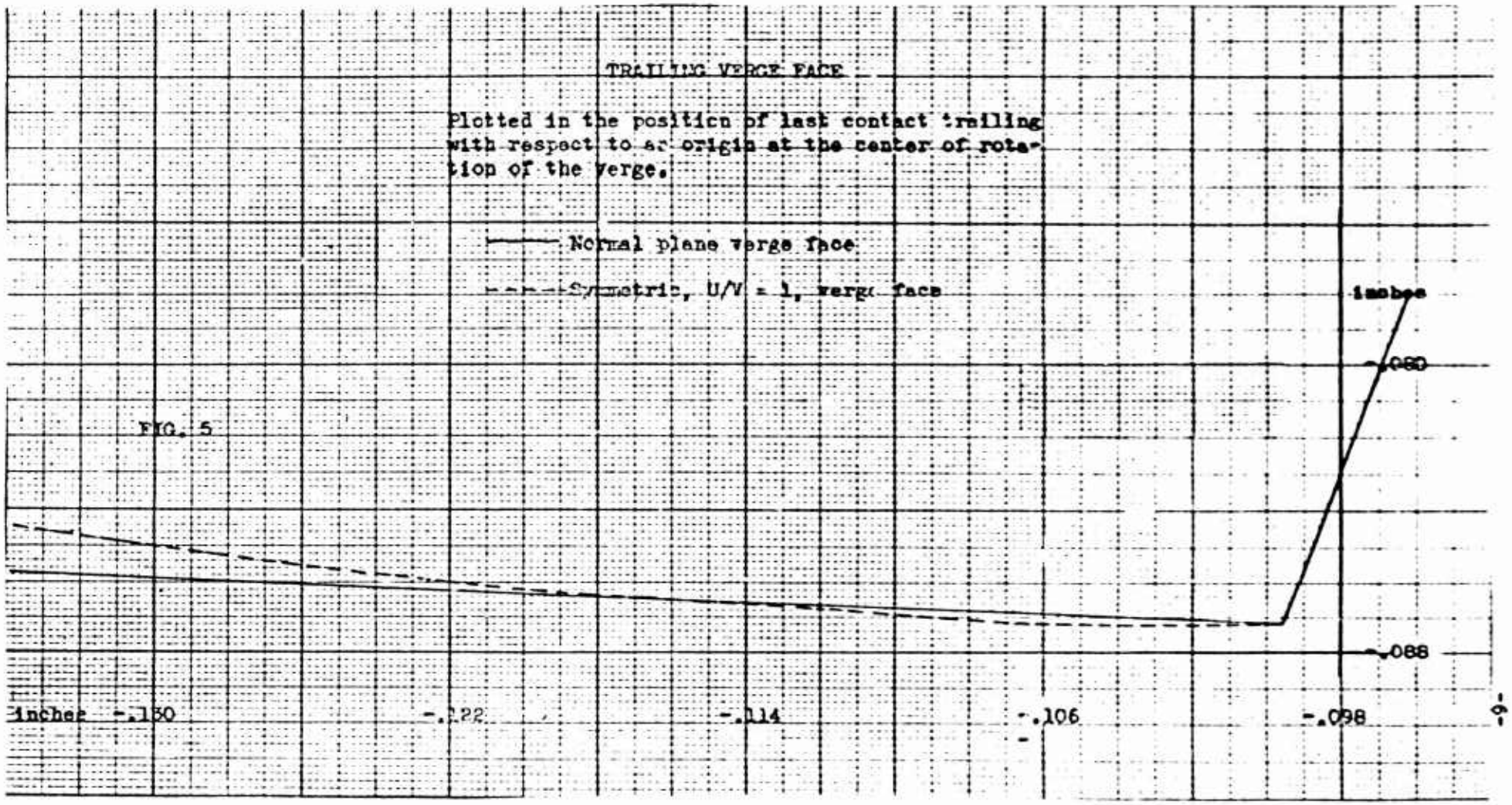
TRAILING VERGE FACE
Plotted in the position of last contact trailing with respect to an origin at the center of rotation of the verge.
Normal plane verge face
Symmetric, U/V = 1, verge face
inches
-.130
-.122
-.114
-.106
-.098
-.088
-.080

FIG. 5

III. THE SYMMETRICAL CYCLE

We next consider the actual cycle of this verge. Since u/v = 1 at all points of contact, leading and trailing, the calculations are considerably simplified. In fact it is possible to derive a set of equations free of the "cut and try" method of preceding reports. This can be done because there now exists a linear relationship between α and θ for each face. This relationship is very simply established in view of the fact that at the leading face $\frac{d\alpha}{d\theta} = +1$, and at the trailing face $\frac{d\alpha}{d\theta} = -1$, as pointed out in the preceding section. In designing the new verge faces it was assumed that the points of last contact (given by α and θ) would be the same as in the normal verge. In the normal verge these are $\theta = .6354$ $\alpha = .0289$ for leading, and $\theta = -.6354$ $\alpha = -.0289$ for trailing. This at once leads to the equations

$$\theta = \alpha + .6065 \qquad \text{leading}$$
$$\theta = -\alpha - .6643 \qquad \text{trailing}$$

Very briefly the equations for the cycle of the u/v = 1 verge are obtained as follows.

The basic differential equation of motion during leading contact (see R-1) becomes

$$-1 = \frac{I_w\dot{\theta} - T}{I_v\ddot{\alpha}} \qquad \text{where } \theta = \alpha + .6065$$

Solving

$$\theta_1 = \frac{1}{2}\frac{T}{I_v + I_w}\, t_1^2 + \dot{\theta}_o t_1 + \theta_o \qquad (1)$$

During free motion leading

$$\theta_2 = \frac{T}{2I_w}\cdot t_a^2 + \dot{\theta}\cdot t_2 + \theta_1$$

and $$\alpha_2 = \dot{\alpha}_1 t_a + \alpha_1$$

while at collision $\alpha_2 = -\theta_2 - .6643$

Solving gives

$$t_a = \frac{-2\dot{\alpha}_1 \pm \sqrt{4\dot{\alpha}_1^2 + \frac{2T}{I_w}(.0994)}}{T/I_w} \qquad (2)$$

From this we can get θ_2 and $\dot{\theta}_2$.

At trailing collision

$$\dot{\theta}_3 = \frac{I_w\dot{\theta} - I\dot{\alpha}_2}{I_w + I_v} \qquad (3)$$

During trailing contact

$$\theta_4 = \frac{\tau}{2(I_v+I_w)} \cdot t_4^2 + \dot{\theta}_3 \cdot t_4 + \theta_3 \qquad (4)$$

During free motion trailing

$$\theta_5 = \frac{\tau}{2I_w} \cdot t_5^2 + \dot{\theta}_4 \cdot t_5 + \theta_4$$

$$\alpha_5 = \dot{\alpha}_4 t_5 + \alpha_4$$

and at collision $\alpha_5 = \theta_5 - .6065$

Solving gives

$$t_5 = \frac{2\dot{\alpha}_4 \pm \sqrt{4\dot{\alpha}_4^2 + \frac{2\tau}{I_w}(.0706)}}{\tau/I_w} \qquad (5)$$

From this we get θ_5 and $\dot{\theta}_5$.

Finally at leading collision

$$\dot{\theta}_6 = \frac{I_w\dot{\theta}_5 + I_v\dot{\alpha}_5}{I_v + I_w} \qquad (6)$$

Equations (1) through (6) give a complete solution for the cycle. Reference to R-1 and R-2 will give the basic information not included here.

In order to determine how this cycle will vary from those studied previously computation is necessary. We shall use the term normal verge to refer to the verge with plane faces whose cycle of motion is asymmetrical. The term symmetrical verge refers to the verge for which u/v = 1 having curved surfaces and resulting in a nearly symmetrical cycle. The untuned clock used in all calculations in this report has the following dynamical constants

$$I_w = 2100 \text{ gmcm}^2 \quad I_v = 2000 \text{ gmcm}^2 \quad \tau = 2.65 \times 10^6 \frac{\text{dyne cm}}{\text{rad.}}$$

Calculations were carried out and cycles plotted for both normal and symmetrical verges, as stated above. The cycles are shown on Fig. 6. The symmetrical verge does not give an entirely symmetrical cycle, although the improvement is marked. Complete symmetry can be achieved only by changing the position of last contact. If the coordinates are leading, $\theta_1 = .6426$, $\alpha_1 = .0361$ and trailing $\theta_4 = -.6426$ $\alpha_4 = -.0217$, true symmetry is achieved. On Figs 1 and 4 these points are marked P^1. It can be seen also that the value of $\bar{\theta}$ is not essentially different for curves 1 and 2. Only in the case of the completely symmetric verge is $\bar{\theta}$ very much changed. Actually, much of this change can be due to the difference in methods used to determine $\bar{\theta}$.

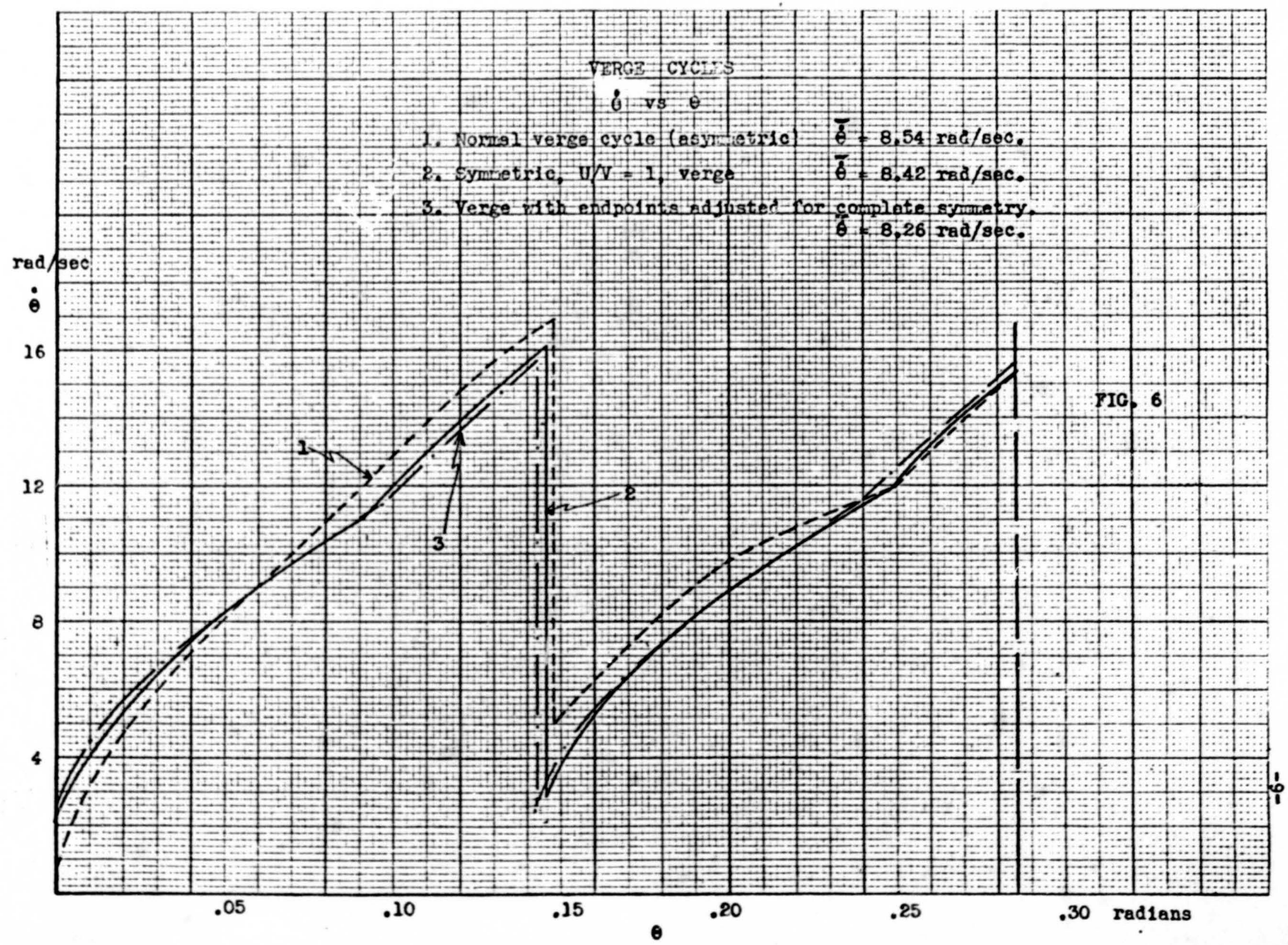
VERGE CYCLES
$\dot{\theta}$ vs θ
1. Normal verge cycle (asymmetric) $\bar{\dot{\theta}}$ = 8.54 rad/sec.
2. Symmetric, U/V = 1, verge $\bar{\dot{\theta}}$ = 8.42 rad/sec.
3. Verge with endpoints adjusted for complete symmetry. $\bar{\dot{\theta}}$ = 8.26 rad/sec.
rad/sec
$\dot{\theta}$
16
12
8
4
1
2
3
.05
.10
.15
.20
.25
.30 radians
θ

FIG. 6

IV. THE EFFECT OF GEOMETRICAL VERGE VARIATIONS ON THE CYCLE

It has been noted that in the normal verge geometrical variations of the leading face have a large influence on the running time, while those of the trailing face are of much less importance. We investigated this situation for the completely symmetrical verge (adjusted end points).

Two possible types of error are considered. The first would result in changing only the point of last contact, and is indicated in Fig 7 (a). Here the error is along a non-contact face of the verge, so that the shape of the face on which the tooth slides is not affected. If the leading tooth is milled as in 3 for example then we simply have a case in which last contact occurs earlier than normal.

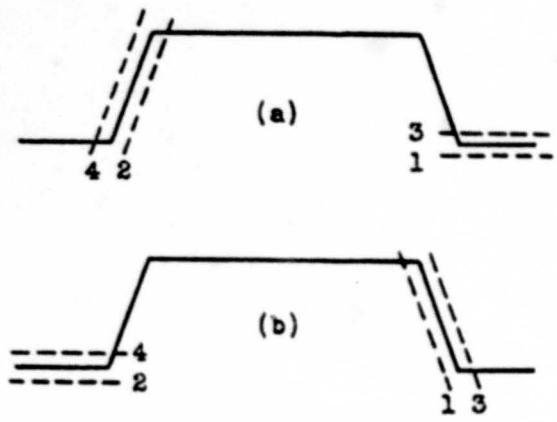

FIG. 7

The second case is that of Fig 7 (b). Here the error is on the contact face itself. The shape is not changed but, as in 4 for example, there is a whole new geometrical situation because essentially the face has been moved over. Calculation similar to that outlined in Section II above enables one to calculate the new geometrical relationships. We find that u/v, although no longer 1, is still very nearly a constant. Cycles are then computed as heretofor described. As a comparision cycle we use curve 3 of Fig 6 for which $\bar{\theta}$ = 8.26 rad/sec. In each case the values of I_w, I_v and τ given above were used. The results are shown in the following tables.

Case (a) (Fig. 7 a)

	Error	$\bar{\theta}$	% variation from symmetrical cycle
1	+ 2 units leading	8.08	2.2%
2	+ 2 units trailing	8.09	2.1%
3	- 2 units leading	8.47	2.5%
4	- 2 units trailing	8.45	2.3%

Clearly the change in $\bar{\theta}$ resulting from these errors is the same at

either face, as is expected in this cycle.

Case (b) (Fig 7 b)

	Error	$\bar{\theta}$	% variation from symmetrical cycle
1	+ 2 units leading	8.50	2.9%
2	+ 2 units trailing	8.55	3.5%
3	- 2 units leading	7.95	3.8%
4	- 2 units trailing	8.02	2.9%

Again, the changes in $\bar{\theta}$ are to an excellent approximation independent of the face on which the error is made.

V. EFFECT OF CHANGES IN k ON THE SYMMETRICAL VERGE CYCLE

Among the geometrical variations found to have an important effect upon the running rate of a clock is the variation in k, the center to center spacing. This variation has been studied in some detail for the normal verge. Reference to R-3 will indicate that k may vary between the limits - .2198 and -.2245 the normal value being -.2222. For the same I_v, I_w and as listed above we determined $\bar{\theta}$ for the extreme values of k, using the normal verge. The results are given in the table at the end of this section.

Next we made similar computations for the symmetrical verge. It is clear from the first that as soon as k changes the value of u/v is no longer 1 nor is it a constant. Furthermore, the method of computing a cycle will be radically changed. A brief outline of this work follows, using the trailing face. Similar considerations hold for the leading face.

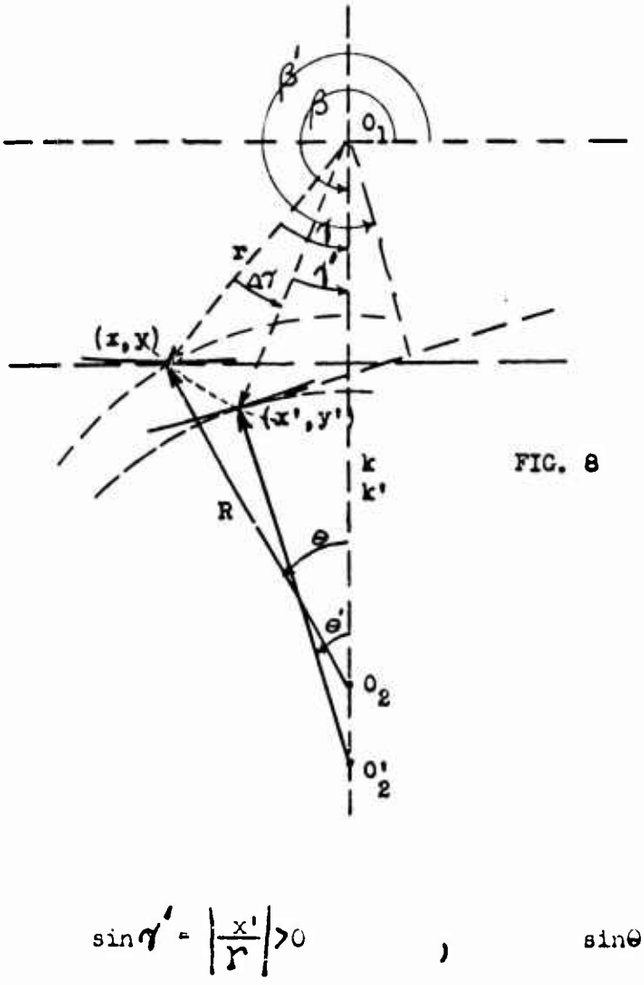

FIG. 8

In Fig. 8 O_1 is the center of rotation of the verge and O_2 that for the starwheel. Point (x,y) is a point of contact between tooth and verge face for the normal value of k. The distance r is no physical dimension of the verge, but represents only the distance from O_1 to the point of contact (x, y). From the diagram

$$r^2 = (R\sin\theta)^2 + (k + R\cos\theta)^2 \qquad k < 0$$

$$\sin\gamma = \left|\frac{R\sin\theta}{r}\right| > 0 \qquad \theta < 0$$

From these equations we may easily find r and γ for each value of θ. Suppose that O_2 is now moved to O' so that $|k'| > |k|$. For the same value of r as above the point of contact has new coordinates (x', y'). These coordinates satisfy the equations

$$x'^2 + y'^2 = r^2$$

$$x'^2 + (y' - k')^2 = R^2 \qquad k' < 0$$

$$\sin\gamma' = \left|\frac{x'}{r}\right| > 0 \quad , \qquad \sin\theta' = \frac{x'}{R} < 0$$

The first two of these equations give us x', and then we find γ' and θ'.

Since

$$\alpha' - \alpha = \Delta\gamma \qquad \text{and} \qquad \beta' - \beta = \Delta\gamma$$

these new coordinates α' and β' can be found.

The equation

$$(u/v)' = \frac{R\cos(\beta' + \theta')}{k'\cos\beta' + R\cos(\beta' + \theta')}$$

gives $(u/v)'$ at once.

The results of this computation are two curves, α' vs θ', $(u/v)'$ vs θ', valid for the value k' used in the equations. Analogous procedure can be used for the leading face. The curves α' vs θ' are straight lines, to an extremely good approximation. The graphs of $(u/v)'$ vs θ' show that $(u/v)'$ is no longer a constant.

Having the above curves enables us to derive equations for solving the cycle. Referring to Section III above, only equations (1) and (4) need be modified in order to obtain the solution. Using the basic differential equation of motion

$$u/v = \frac{I_w \ddot{\theta} - \tau}{I_v \ddot{\alpha}}$$

one easily finds $\ddot{\theta} = f(\theta)$, which is plotted on a graph. This curve may be approximated very closely as a 4th order polynomial. $\dot{\theta} = f(\theta)$ is immediately integrable by elementary methods, and $\dot{\theta}_1$ is obtained. Similar considerations hold for the trailing case.

Cycles were computed for three different values of k, first for the normal verge and then for the "u/v = 1" verge, where of course u/v is no longer unity. The results are shown in the following table. The verge starwheel combination is the same as that described in Section III above.

k	Type Verge	$\bar{\dot{\theta}}$	% variation from normal
-.2198	Normal	7.93	7.1%
-.2222 (Normal)	Normal	8.54	----
-.2245	Normal	9.18	7.5%
-.2198	Symmetric	7.77	7.7%
-.2222	Symmetric	8.42	----
-.2245	Symmetric	9.02	7.1%

It is clear that although the % variation introduced into $\bar{\dot{\theta}}$ by changes in k is not improved by using the symmetric verge, neither is is made any worse.

VI. CONCLUSION

The problem of reducing the variation in running times among a large number of clocks is only partly a problem of geometry of course. The friction effects which vary so greatly from one mechanism to the next are very probably the most important single factor involved. This report presents no definite results in regard to the geometrical effects. Verges for which u/v = constant can be designed. Theoretically, such verges respond similarly to geometrical variations at either face. The importance of the leading face so clearly evident for the normal verge, is conspicuously absent here. Variations in center to center distance cause no greater changes in running times than in the normal verge. It would appear that some possible improvement in obtaining uniform running rates might result from the redesign of the verge faces,

PART II. AN EXPERIMENTAL STUDY OF THE MOTION OF AN UNTUNED CLOCK

SECTION VII: INTRODUCTION

It was felt that a study of the relationship between the starwheel and verge in the actual clock mechanism might provide some useful information. In order to discover experimentally this relationship, the starwheel and verge were insulated from each other and, in effect, the variation in capacitance between the two was observed. Since the capacitance between the starwheel and verge is here predominantly a function of their separation, a study of the results should reveal information concerning the nature of the relative motion between the two parts.

In the following description of the experimental work performed, computations of the relative time occupied by the various contact and free time periods are carried out; however, no other attempts at quantitative interpretations were made.

SECTION VIII: THE APPARATUS

The determination of the starwheel-verge capacitance variation was centered about the circuit shown in Figure 9. This consists of a tuned grid-tuned plate oscillator coupled to the input of an infinite impedance detector; the input of the detector is then subjected to a single stage of amplification before being fed into the vertical amplifier of a Tektronix 514-D cathode ray oscilloscope.

The resonant frequency of the fixed oscillator grid tank circuit is approximately 2.8 mc. The oscillator plate tank and the detector grid tank are tunable, and the coupling between the oscillator and detector stages is adjustable; the result is that the amplitude of the oscillation is readily variable.

A peak voltage output of approximately 25 volts is available from the amplifier stage. The filament and plate voltages are variable in order to aid in obtaining the correct amplitude signal at the oscilloscope. A block diagram of the equipment employed is shown in Fig 10.

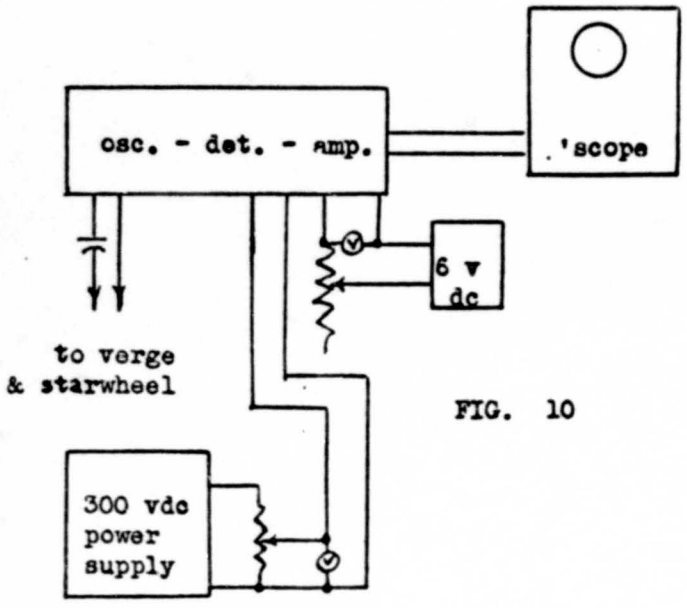

FIG. 10

The starwheels and verges being tested were mounted in a rebuilt clock mechanism in which the starwheel bearings were insulated from the verge bearings. The verge was then connected to the grid of the oscillator tube, and the starwheel was connected to the plate through a very small capacitance made by twisting together two two inch insulated wires.

Since in effect the starwheel-verge combination and the twisted wire capacitor are two capacitors connected in series between the plate and the grid of the oscillator, as the starwheel and the verge approach each other the total capacitance increases, reaching a maximun when the starwheel and verge are in contact, this equilibrium value being the capacitance of the twisted wires. (See Fig. 11). This increased capacitance causes an increase in the amplitude of oscillation of the 605 oscillator. This is transmitted to the detector as a modulated RF signal.

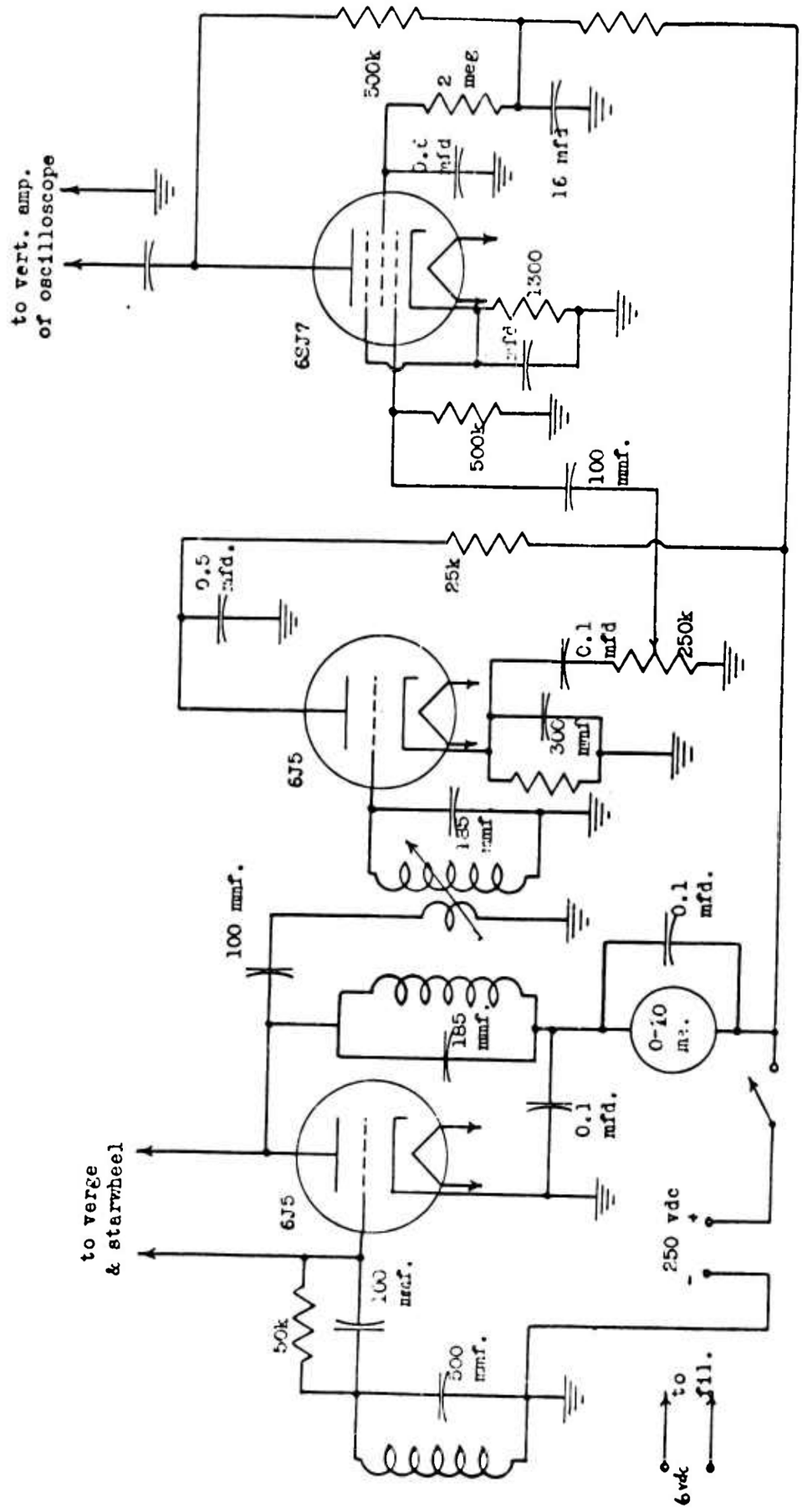
to vert. amp.
of oscilloscope
500k
2 meg
16 mfd
6SJ7
1300
500k
100 mmf.
25k
0.5 mfd.
6J5
0.1 mfd
250k
300 mmf
185 mmf.
100 mmf.
0.1 mfd.
185 mmf.
0-10 ma.
0.1 mfd.
to verge
& starwheel
6J5
250 vdc
50k
100 mmf.
500 mmf.
6 vdc
to fil.

FIG. 9

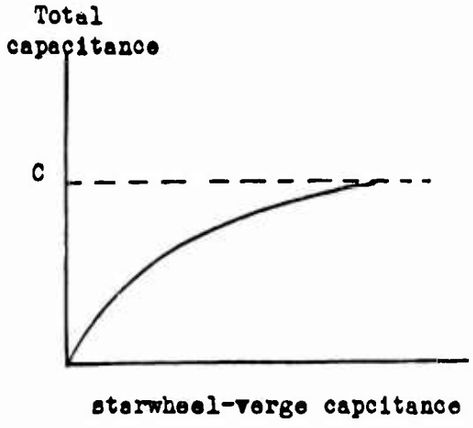

FIG. 11

In the actual experimental runs that were made, the oscillator was adjusted so that it was oscillating very weakly; the oscillator in this condition is most sensitive to variations in grid-plate capacitance. As the untuned clock was allowed to unwind, a lever attached to the winding arm tripped a micro switch which in turn actuated a single horizontal sweep across the oscilloscope tube. The resulting trace was then photographed.

SECTION IX. RESULTS

As in previous experimental work performed on the actual mechanism in this laboratory, most of the work described below was done with the one second clock. Even though some of the results for other clocks(0.5 sec, 1.5 sec, 10 sec, etc) are somewhat different, the following description leads to an understanding of the method employed.

Photographs of thirty-nine complete equilibrium cycles for the nominal one second clock were obtained. Several qualitative characteristics of the cycles were immediately apparent. First of all, it was seen that a true "sliding contact" between verge and star wheel never occurred; rather, contact periods were presented as series of very rapid oscillations of the trace-apparently rapid "bounces" of the verge and starwheel. The true dynamical significance of these "bounces" has not been investigated in detail.

In addition, a striking difference between the nature of leading contact and that of trailing contact was noted. In all cases, the leading contact period was composed of two short "periods of contact" with a short "free time" separating them. However trailing contact was made up of from one to four individual contact periods.

For convenience of discussion, the complete equilibrium cycle will henceforth be divided into six portions:

1. First Leading Contact Period
2. Leading Contact Free Time
3. Second Leading Contact Period

} Referred to in R-1 as "Leading Contact Period"

4. Leading Free Time
5. Trailing Contact

} Composed of from one to four individual contact periods

6. Trailing Free Time

The time occupied by each of the above named "periods" was computed for each of the thirty-nine cycles as a percent of the total time elapsed during that complete cycle. The mean percent time for each period was then computed by plotting a mean distribution curve. The resulting "average"cycle may then be described as follows:

First Leading Contact	19.2% ± 3.4%		
Leading Contact Free Time	12.0% ± 2.3%	38.8%	51.3%
Second Leading Contact	7.6% ± 1.9%		
Leading Free Time	12.5% ± 3.5%		
Trailing Contact	41.3% ± 2.4%		48.7%
Trailing Free Time	7.4% ± 1.5%		

The times for each period were expressed as a percent of complete cycle because of the fact that the cycle length varied because of variations in friction between trials. It is to be remembered that the trailing contact period was composed of varying numbers of individual contact periods, but that they were lumped together for convenience in calculation.

In Figure 12 is shown a typical trace obtained from the apparatus. Two complete cycles are shown. Note that the "contact periods" are composed of many rapid bounces. Furthermore the two trailing contact periods are entirely different in nature from each other; that is, the first trailing contact period shown is seen as one single period of contact; the second is composed of four individual contact periods.

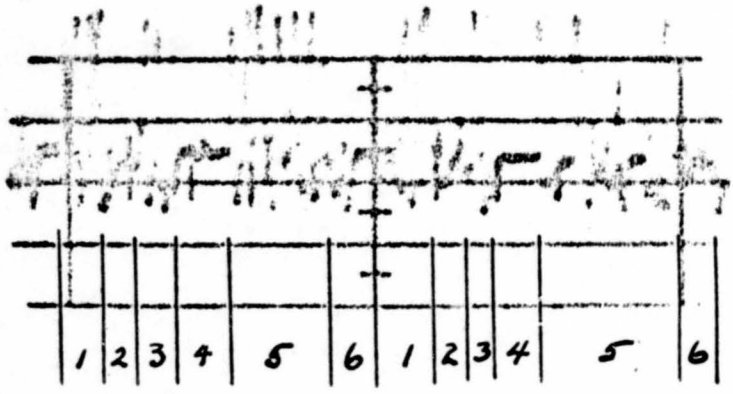

FIG. 12

SECTION X. CONCLUSIONS

It is seen that the nature of the relationship between the star-wheel and verge is quite different from what is assumed in the theoretical work. In the nominal one second clock, no pure sliding contact ever occurs; furthermore, the periods formerly referred to as leading contact and trailing contact are made up of several smaller contact periods.

The experimental work described does certainly point to a difference in the nature of trailing and leading contact; this is very probably closely related to the known fact that the leading face is very sensitive to geometrical changes, as compared to the trailing face.